

Novel P(3HB) Composite Films Containing Bioactive Glass Nanoparticles for Wound Healing Applications

Lydia Francis^a, Decheng Meng^c, Ian.C. Locke^a, Jonathan Knowles^d, Nicola Mordan^d, Vehid Salih^d, Aldo.R.Boccaccini^{b,c*} and Ipsita Roy^{a*}

* **Correspondence to: Prof Ipsita Roy**, Faculty of Science and Technology, University of Westminster, 115 New Cavendish Street, London W1W 6UW. royi@wmin.ac.uk and royips@gmail.com.

Prof Dr.-Ing. habil. A. R. Boccaccini, Head, Institute of Biomaterials Department of Materials Science and Engineering, University of Erlangen-Nuremberg, Cauerstr. 6, 91058 Erlangen, Germany. aldo.boccaccini@ww.uni-erlangen.de

- a) Faculty of Science and Technology,
University of Westminster,
115 New Cavendish Street, London W1W 6UW
- b) Department of Materials, Imperial College London
Prince Consort Rd.
London SW7 2BP
- c) Institute of Biomaterials, Department of Materials Science and Engineering,
University of Erlangen-Nuremberg,
Cauerstr. 6, 91058 Erlangen, Germany
- d) UCL Eastman Dental Institute,
University College London,
256 Gray's Inn Road,
London WC1X 8LD

Abstract

Bioactive glass (BG) is considered an ideal material for haemostasis as it releases Ca^{2+} ions upon hydration, which is required to support thrombosis. In this study the effect of the presence of the BG nanoparticles in P(3HB) microsphere films on the structural properties, thermal properties and biocompatibility of the films were studied. The nanoscaled bioactive glass with a high surface area was also tested for its *in vitro* haemostatic efficacy and was found to be able to successfully reduce the clot detection time. In an effort to study the effect of the roughness induced by the formation of HA on the cellular functions such as cell adhesion, cell mobility and cell differentiation, the composite films were immersed in SBF for a period of 1, 3 and 7 days. From the SEM images the surface of the P(3HB)/n-BG composite microsphere films appeared fairly uniform and smooth on day 1, however on day 3 and day 7 a rough and uneven surface was observed. The presence of HA on the composite microsphere films on day 3 and day 7 influenced the surface roughness of the films. However, when the P(3HB)/n-BG

composite microspheres with enhanced surface roughness were tested for biocompatibility, reduced amount of protein adsorption and cell adhesion were observed. This study thus revealed that there is an optimal surface roughness for the P(3HB) microsphere films for increased cell adhesion, beyond which it could be deleterious for cell adhesion and differentiation.

Keywords n-BG, P(3HB) microspheres, n-BG/P(3HB) composite films, bioactive glass, surface roughness, cell response, wound healing.

Introduction

A widespread need for the development of new biomaterials that can interface with soft biological tissues and the improvement of existing materials to promote skin tissue regeneration is emerging.¹ Skin comprises a major part of the body, any damage due to injury, burns and disease can have a major physiological or functional consequence. Therefore, several acute and chronic skin wounds are being treated using various tissue engineered skin substitutes.^{1, 2} The current solution involves grafting of cadaveric skin. However this approach is plagued with problems such as disease transmission and immune response.³ Dermal scaffolds from animal sources have also been used to promote the regenerative process in many reconstructive surgical procedures. However before using these scaffolds they have to be decellularised using different reagents and one of the main challenges facing their use is the effect of these reagents on the extracellular matrix (ECM) such as collagen and glycosaminoglycans needed for tissue regeneration.⁴

In tissue engineering, a biomaterial is designed that can be used to replace the damaged organ or tissue. However for skin tissue regeneration or wound healing, the biomaterial should possess the strength to promote cell migration and growth of skin cells such as keratinocytes, melanocytes and fibroblasts.^{1, 2} They should be non-toxic, non-antigenic and facilitate angiogenesis while being incorporated with minimal scarring and pain. In addition to this, biomaterials are also required to act as an artificial extracellular matrix (ECM) for the cells to attach. Therefore, combinations of natural and synthetic polymers have been used to address this problem. Genzyme developed an epithelial skin replacement (Epicel) which consists of a polyurethane sheet with keratinocytes to form colonies or fully confluent cells. Although Epicel promoted the formation of a new epithelium, the polymer was only used as a support for cell growth and not as a scaffold for tissue regeneration.³ Other materials such as Dermagraft was developed using a combination of human foreskin fibroblasts grown on poly(lactide-co-glycolide) PLGA scaffolds. Although both mechanical stability and tissue regeneration was achieved, the rate of PLGA degradation could not be controlled and the extracellular matrix content, cell morphology and assembly could not be supported.³ Since these materials were unable to support appropriate cellular activity such as the molecular signalling cascades which prevented the clinicians from manipulating it in a surgical setting, other replacements such as biodegradable polyhydroxyalkanoates are being considered for skin tissue engineering/regeneration.¹ P(3HB) from Gram positive bacteria lack immunogenic properties

and hence are excellent materials for medical applications. They also exhibit biocompatible properties as well as support cell growth. The degradation products extracted in buffer solutions at 37 °C are significantly less bioactive and acidic when compared to glycolic acids and lactic acids.⁵ When mouse glial cells were cultured with P(3HB), the end products from the degradation of P(3HB) was found not to be harmful.⁶ Similarly human epithelial cells adhered and spread well when cultured on P(3HB) fibres pre-treated with strong acid or base and used as wound dressings.⁷

Since P(3HB) can be fabricated into any complex shape and structure, it has been combined with bioactive ceramics. A number of synthetic biodegradable polymers and bioactive ceramic scaffolds have been made but they could not be used *in vivo* as they provoked an adverse tissue response due to their acidic degradation products.⁸ Several inorganic materials which were previously used only for applications such as bone and dental repair are now being considered for other applications such as wound healing. During a traumatic injury, the body's skin barrier is breached which results in haemorrhage.⁹ The lack of covering of the wound can result in infection, in turn leading to further complications. However, traditional dressings may be insufficient to control the haemorrhage.⁹ Currently zeolite-based granular materials are used on the surface of wounds to induce rapid clotting. Zeolite is a haemostatic agent, which has a high affinity for water; therefore it has a concentrating effect on the plasma by selectively dehydrating the blood. However, as a consequence of the affinity for water, energy release is very high during hydration; due to which they tend to burn the surrounding healthy tissues.⁹ Therefore; efforts have now been focused in developing new biocompatible materials to serve as scaffolds with an ability to induce haemostasis as well as promoting tissue regeneration.

Although bioactive glass ceramics were used largely for dental and bone applications, researchers like Ostomel⁹ have focused on the use of these silicate glasses for blood clotting applications. The authors formulated a high surface area bioactive glass and then tested its *in vitro* haemostatic efficacy. Haemostatic bioactive glass (BG) was considered as an ideal material for haemostasis as it is known to release Ca²⁺ ions upon hydration, which is required to support thrombosis.⁹ In another study Ostomel⁹ suggested factors such as porosity, Si/Ca ratio and the spherical morphology of bioactive mesoporous glass microspheres (MBGMs) as important properties that affect the biological response required for wound healing. In addition, during clotting, the intrinsic pathway of the blood clotting cascade is activated by the polar surfaces of the glasses. When blood is exposed to a foreign polar surface, blood-clotting

factors such as Factors XII, XI, prekallikrein and high molecular weight kininogen are initiated. The activated factors are then responsible for the activation of the thrombin enzyme and polymerization reaction of fibrin. During haemostasis a platelet plug is formed at the site of injury, while the procoagulant substances activated in this process are localized at the site of injury.¹⁰ Ostomel⁹ also found that the high surface area of the bioactive glass could provide the support needed for thrombosis as well as provide an optimum ratio of SiO₂ to Ca²⁺ ions required for the clotting cascade. The *in vitro* haemostatic efficacy can be tested using a thromboelastograph (TEG), which monitors the change in the viscoelasticity of blood, in the presence of the haemostatic agent during thrombosis and thrombolysis.⁹

In this work, for potential application in wound healing, nanoscale bioactive glass particles (n-BGs) were incorporated within a biodegradable polymer P(3HB) matrix. The chemical composition of the n-BG used was not very different from the commercially available 45S5 Bioglass[®] microscale bioactive glass particles (m-BGs); however, the n-BG used were spherical in shape with a uniform surface morphology as compared to the (m-BGs), which are irregular in size with large agglomerates.¹¹ The spherical morphology of the ceramic particles with a high specific surface area is crucial for interface effects such as hydroxyapatite (HA) formation and contact activated coagulation.^{9,11} The presence of nanoscale particles have been found to have an effect on the microstructural, mechanical and *in vitro* degradation behaviour of the composite systems used in tissue engineering applications.¹³ The amount of nBG present can be used to regulate the degradation behavior of the composites and also the 3-hydroxybutyric acid produced as a result of degradation can be neutralized by the alkaline dissolution products of nBG.

Cell response is affected by a number of physicochemical factors such as surface energy, surface charge and chemical composition of the biomaterials. Apart from these factors, cell response is also affected by surface topography.¹³ Surface topography is the most decisive physical cue for the cells, as the topography can be used to guide the cell orientation to achieve functional tissue such as tendons and nerves. Researchers have focused their efforts in trying to mimic nanoscale topographical features found in the tissue, in the hope that these features can promote cellular functions such as cell adhesion, cell mobility and cell differentiation.¹⁴

Nanoscale features are known to have both a direct influence and an indirect influence on the conformation of the adsorbed extracellular matrix components. Cell adhesion on the

nanotopographical substratum is dependent on integrin adhesion as well as the topographical nanofeatures. During cell adhesion, transmembrane proteins called integrins are recruited and activated. Integrins are known to establish the initial cell-matrix interactions. Integrin receptors are also known to form adhesion plaques or focal adhesion sites on the substratum. Following the formation of focal adhesion sites, events such as integrin clustering occurs. Therefore, for an increased cell adhesion, the lateral spacing in the nanofeatures of the matrix must be around 15-30nm.¹⁵ Nanofeatures such as height, diameter and edge-edge spacing are also known to affect the integrin clustering. Several polymeric substrates with nanotopographical features have shown an increase in cell adhesion. For example, poly(L-lactic acid) films with nanofeatures of 500-550 nm in diameter and 250-300 nm in height displayed an increase in human foreskin fibroblast adhesion.¹⁶

The sub cellular structures of the single cells such as cytoskeletal elements, transmembrane proteins and filipodia of the cells, which are tens of microns in diameter, tend more towards the nanoscale features.^{17, 18} Several techniques such as electron beam lithography, photolithography have been used for creating ordered features and phase separation and colloidal lithography have been used to create unordered surface patterns. However, apart from using these techniques, other nanophase materials such as HA nanoparticles, bioactive glass nanoparticles and stimuli-sensitive polymeric nanoparticles have been used to produce nanometer features. These nanophase materials have displayed several advantages such as enhanced cell adhesion, proliferation and bioactivity.¹⁹

It has been observed that the presence of nanoscale bioactive glass particles affects the microstructural, mechanical and biological properties of composite films used for bone tissue engineering applications. However, previous research using P(3HB) as a matrix have considered only films. Microspheres made of P(3HB) are highly interesting as carriers of drug and bioactive particles. This is the first time, the use of P(3HB)/nanoscale bioactive glass (n-BG) composite microspheres compressed to form films have been used for applications in wound healing. In addition, in this work, for the first time, n-BG particles have been used to investigate their haemostatic efficacy in wound healing applications due to their high surface area which could provide the support needed for thrombosis as well as the release of an optimal ratio of SiO₂ to Ca²⁺ ions required for the clotting cascade. Hence, in this work, P(3HB) has been combined with n-BG to form multi-functional scaffolds. These composite films were additionally immersed in simulated body fluid (SBF) for a fixed time period in order to induce

the formation of HA on the surface of the composite films, leading to the formation of P(3HB)/n-BG surface functionalized composite films.

In the first part of this study, n-BG particles were mixed with the polymer solution, made into microspheres and compressed into films followed by a complete characterization of the composite films. The results can be categorized as (i) the effect of n-BG particles on the structural and thermal properties (ii) the effect of n-BG particles on surface mediated phenomena such as haemostatic activity. (iii) A comparative study on the *in vitro* biocompatibility of P(3HB) and P(3HB)/n-BG microsphere films using the HaCaT (keratinocyte) cell line.

In the second part of this study, the P(3HB)/(n-BG) microsphere films were immersed in simulated body fluid (SBF) for a fixed time period to induce the formation of HA on the surface of the composite films, leading to the formation of surface functionalized films. These P(3HB)/n-BG composite films with HA deposition were also assessed in order to understand the effect of HA deposition on the biomaterial's surface properties, on protein adsorption as well as on keratinocyte adhesion and viability.

The optimal surface nano-topography of P(3HB)/n-BG microspheres films can be engineered by immersion in SBF, which is used as a route for functionalization. Once the formation of HA which is known to mimic nanoscale topographical features that promote cellular functions such as cell adhesion, cell mobility and cell differentiation required for wound healing are achieved, the composite patch would be implanted *in vivo* by placing them on the wound bed as a dermal graft. Polymers are known to be more conducive to dermal tissue regeneration *via* chemical signals or biological signals known to induce dermal regeneration and repair. Thus these novel scaffolds would be used to induce cell attachment, haemostasis, as well as to provide mechanical support to promote tissue regeneration.

Experimental Section

Materials

Fabrication of Poly(3-hydroxybutyrate)/nanobioglass (P(3HB)/n-BG) composite microsphere based films.

Nanoscale bioglass (n-BG) particles were used in this study to prepare the composites. These n-BG particles were fabricated by the flame spraying method as described in Misra *et al.*, 2007.¹⁶ Appropriate amounts of n-BG particles were added to the polymer solution (1g of P(3HB) dissolved in 8 mL of chloroform) to yield composites with 10 wt% n-BG in the P(3HB) matrix. This mixture was further sonicated for 1-2 min (Ultrasonic Homogenizers US200, Phillip Harris Scientific, UK) to improve the dispersion of the n-BG particles by segregating possible agglomerations. The P(3HB)/n-BG mixture was then transferred into 40 mL of 1% (w/v) aqueous polyvinyl alcohol (PVA) solution, and stirred at 800 rpm for 3 minutes. This solution was then added to 500 mL of 0.5% (w/v) aqueous PVA solution, forming the second-oil-in-water emulsion. The microsphere fabrication method has been described previously Francis *et al.*, 2010.³² 0.1g of the P(3HB) microspheres with n-BG were uniaxially compressed to form a disc using a hydraulic hand press and a force of 0.09MPa to the films of diameter, 12.87mm, thickness, 0.87mm and surface area of 1.13cm².¹⁰

P(3HB) and P(3HB)/n-BG composite microsphere films immersed in SBF

The components of Simulated Body Fluid (SBF) *i.e.* sodium chloride 15.92g, sodium bicarbonate, 0.72g; potassium chloride, 0.44g; potassium phosphate dibasic trihydrate 0.45g; magnesium chloride hexahydrate, 0.61g; calcium chloride, 0.55g; sodium sulphate, 0.142g; TRIZMA[®] base, 12.11g; hydrochloric acid -appropriate amount to adjust the pH to 7.25 were dissolved in 2L of final volume of deionized water and the pH adjusted to 7.25. Freshly prepared SBF was used for all the analysis and when needed, was stored at 4°C for no more than 14 days. The samples were kept in a 37°C incubator under static conditions and at desired time points samples were collected, gently washed with deionized water and left to dry overnight at 37°C in an incubator. The (P(3HB) and P(3HB)/n-BG composite microsphere films were collected after 1, 3 and 7 days of incubation, washed with deionized water and vacuum-dried before further examination.

Thromboelastograph (TEG) studies

The haemostatic efficacies of the n-BG particles were measured using a thromboelastograph (TEG) haemostasis analyser 5000 at St Thomas' Hospital, London U.K. In a TEG, the polyethylene cup containing blood is rotated $\pm 5^\circ$ around a torsion wire. The time until the bimodal symmetric viscoelasticity curve's amplitude is 2 mm is referred to as R (min) and

represents the initial detection of clot formation. The maximum separation of the curves is referred to as MA and represents the maximum clot strength (dyn/cm^2).⁹ Kaolin a standardised reagent consisting of kaolin, buffered stabilizers and a blend of phospholipids was used for this study. Kaolin containing vials were warmed to room temperature initially. The vials were gently tapped and 1.0 mL of native blood was added into each vial and then gently inverted for a few times. Then 340 μL of the citrated blood was added into TEG analyser cups containing 20 μL of 0.2M calcium chloride. The lever was moved to the start position and the test and sample run were carried out until the MA parameter was defined. The TEG analyser was connected to a computer running the TEG analytical software (Haemoscope Corporation).

Scanning electron microscopy/Energy Dispersive X-Ray analysis (SEM/EDX)

Microstructural observations of P(3HB)/n-BG composite microsphere films were performed using a JEOL 5610LV scanning electron microscope. Scanning electron microscopy (SEM) was also used to characterize the changes that occurred on the scaffold surfaces upon immersion in SBF. The increase in the amounts of phosphorus (P) and calcium (Ca) and the decrease in the amounts of sodium (Na) and silicon (Si) were detected by energy-dispersive X-ray (EDX) analysis. EDX spectra of the composite samples were taken at different time points of immersion in SBF. These measurements were carried out at 10 kV in a field emission (EDX, INCA Oxford).

X-ray diffraction analysis (XRD)

X-ray diffraction (XRD) analysis on P(3HB)/n-BG microsphere films were performed on a Brüker D8 Advance diffractometer in flat geometry, using Ni filtered Cu $K\alpha$ radiation. Data were collected from 10 to 100° in θ - θ mode with a primary beam slit size of 0.6 mm. The analytical parameters were the following: step size 0.04°, scan step, time of 1s, and diffraction range 5-55° (2θ)

Differential Scanning Calorimetry (DSC)

The thermal properties of P(3HB)/n-BG microsphere films retrieved at different time points after water uptake studies were measured using a Perkin-Elmer Pyris Diamond DSC (Perkin-Elmer Instruments, USA). The sample masses for each of the measurements were in the range

of 5-7mg. The samples were encapsulated in standard aluminum pans and all tests performed under nitrogen atmosphere. The samples were heated/cooled/heated at a rate of $20^{\circ}\text{C min}^{-1}$ between -50°C and 250°C . All measurements were carried out in triplicates.²⁰

White light interferometry

2D and 3D plots of the surface topography were obtained by the means of white light interferometry (ZYGO[®], New View 200 OMP 0407C, UK) in order to evaluate the topography and measure the surface roughness of the samples. P(3HB) and P(3HB)/n-BG microsphere films were analyzed at 10 x magnifications using a $100\mu\text{m}$ bipolar scan. Three analyses per sample were performed to get an average root mean square (rms) measurement.

Water contact angle study

Static water contact angle measurements of the P(3HB)/n-BG composite microsphere films were carried out in order to evaluate the wettability of the samples. The experiment was carried out on a KSV Cam 200 optical contact angle meter (KSV Instruments Ltd., Finland). An equal volume of water ($<12\mu\text{L}$) was placed on every sample by means of a gas light micro-syringe forming a drop. Photos (frame interval-1s, number of frames-20) were taken to record the shape of the drops. The water contact angles on the specimens were measured by analyzing the record drop images (n=3) using the Windows based KSV-Cam software.

Protein adsorption test

The protein adsorption study was carried out by placing the P(3HB)/n-BG composite microsphere films and the composite scaffolds covered with HA in 2 mLs of cell culture media (Dulbecco's Modified Eagle Medium supplemented with 10% fetal calf serum, 2mM L-glutamine, and 1% (w/v) penicillin and 1% (w/v) streptomycin solution), at 37°C for 24 h to determine the amount of protein adsorbed on the surface. After 24 h the samples (were washed with Hank's balanced salt solution, pH 7.4. The samples were then treated with 1mL of 3% Triton X-100¹³. The total amount of protein adsorbed was quantified using a bicinchoninic acid (BCA) reagent kit (Thermo scientific). The optical density of the samples was measured at 562 nm using a standard spectrophotometer (Novaspec II Visible spectrophotometer, UK) against a calibration curve using bovine serum albumin (BSA), as per

the manufacturer's protocol. The total amount of protein adsorbed on the surface of the samples was normalized for the surface area.

Cell culture studies on P(3HB/n-BG composite microsphere films

All media including buffers, trypsin and dyes were filter-sterilized prior to use and warmed to 37 °C. The human keratinocyte cell line (HaCaT) was grown in Dulbecco's Modified Eagle Medium (DMEM), supplemented with 10% fetal calf serum, 2mM L-glutamine and 1% (w/v) penicillin and 1% (w/v) streptomycin solution. The medium was changed every 2 days. The cell cultures were maintained at 37°C, 5% CO₂ and passaged on confluence by trypsin treatment. Following cell detachment, fresh medium was added to the cell suspension, which was then centrifuged at 500g for 10 minutes. The resulting cell pellet was resuspended in fresh medium and transferred to 75 cm² tissue culture flasks as required.²²

Cell seeding on substrates

All samples were sterilized using ultra-violet (UV) light. The samples were kept in 24-well microplates and placed under UV for 30 minutes, for each side of the sample. This form of sterilization was employed as it has been shown to be effective compared to washing with alcohol or autoclaving.²³ The semi-confluent HaCaT cells were released from the flasks by trypsinisation and concentrated to pellet form by centrifugation (1317g, 5 min). A cell seeding density of 20,000 cells/cm² was used for the films. The samples were placed in a polystyrene 24 well flat bottomed tissue culture plate with the film samples placed in the centre of the well and 2 mLs of the cell suspended media were added for attachment of the keratinocytes. The plates were incubated in a humidified environment (37°C, 5% CO₂) for a period of 3 days. Standard tissue culture plastic was used as the control surface. Neutral Red (NR) assay was used to assess cell viability.²²

Neutral Red assay

The cell attachment study was carried out using the Neutral Red (NR) assay.²² Briefly, the films were incubated with 2 mL of media containing 40 mg/mL of NR, which was filter-sterilized. The growth on the standard tissue culture plate was used as control. The 24 well plates containing the films were then further incubated for 3 h at 37°C to allow for uptake of the dye

by viable, uninjured cells. The NR containing medium was removed after 3 h and the films gently removed and placed in another 24 well plate. The films were then quickly washed with 200 μL of fixative (1% CaCl_2 -0.5% formaldehyde). Next, 200 μL of another solution containing 1% acetic acid and 50% ethanol solution was added to each well to extract the dye. The plates were then allowed to stand at room temperature for 10 minutes, followed by rapid agitation on a microtitre plate shaker. The absorbance of the extracted dye (100 μL) was read at 540 nm on a Thermomax microtitre plate reader (MDS Analytical Technologies (UK) Ltd., Wokingham, UK). All experiments were performed at least three times. The total NR uptake is directly proportional to the number of live, uninjured cells. Control plates containing only cells and medium were run alongside every experiment²². The percentage cell viability was calculated as follows:

$$\% \text{ Cell viability} = \frac{\text{Mean absorbance of the cells on the composite microsphere films}}{\text{Mean absorbance of the cells on the tissue culture plates}} \quad (1)$$

All NR assay values were expressed as a percentage of the growth on the tissue culture plate. The baseline of 100% viability was set as the absorbance of the test cells. Background absorbance due to non-specific reactions between the test materials and the NR dye were deducted from the exposed cell values. The difference in the surface areas of the tissue culture plastic (1.86 cm^2) and the films (1.13 cm^2) were considered and the correction factor was applied to determine the % cell viability on the films.

Scanning Electron Microscopy (SEM) to observe cell attachment

P(3HB)/n-BG composite microsphere films were examined under SEM to observe the HaCaT cell attachment and spreading on the surface of samples. Specimens from Day 1 and Day 3 were fixed in 3% glutaraldehyde in 0.1 M cacodylate buffer for 12h at 4°C. Subsequent dehydration using a series of graded ethyl alcohols (50%, 70%, 90% and 100%) was performed. Samples were then critical point dried by immersion in hexamethyldisilazane for 2 min and left in a fume cupboard for 2h. The dried samples were then attached to aluminum stubs, gold coated and examined under SEM (JEOL 5610LV, USA) at various magnifications.

RESULTS AND DISCUSSION

Nanoscale bioactive glass (n-BG), P(3HB) microspheres and P(3HB)/n-BG composite microspheres characterizations.

The nanoscale bioactive glass (n-BG) particles used in this study were spherical in shape with relatively small agglomerate sizes as seen in Fig 1A. These n-BG particles had a specific surface area (SSA) of $79 \text{ m}^2\text{g}^{-1}$ and a mean diameter of 29 nm .³ The P(3HB) microspheres (Fig1B) had a mean diameter of $2 \mu\text{m}$ and a SSA of $6.05 \text{ m}^2\text{g}^{-1}$. The surface morphology of P(3HB) microspheres as observed by SEM (Fig 1B), also appeared spherical in shape, with a smooth surface morphology. These microspheres were prepared by the solid-oil-in-water (s/o/w) technique. The microsphere fabrication method has been described previously Francis *et al.*, 2010.³² The P(3HB)/n-BG composite microspheres had a mean diameter of $1.7 \mu\text{m}$ and exhibited a SSA of $9.4 \text{ m}^2\text{g}^{-1}$. SEM images of the composite microspheres (Fig 1C), revealed smooth surfaces as well as the presence of agglomerations of the n-BG particles present on the surface of the microspheres.

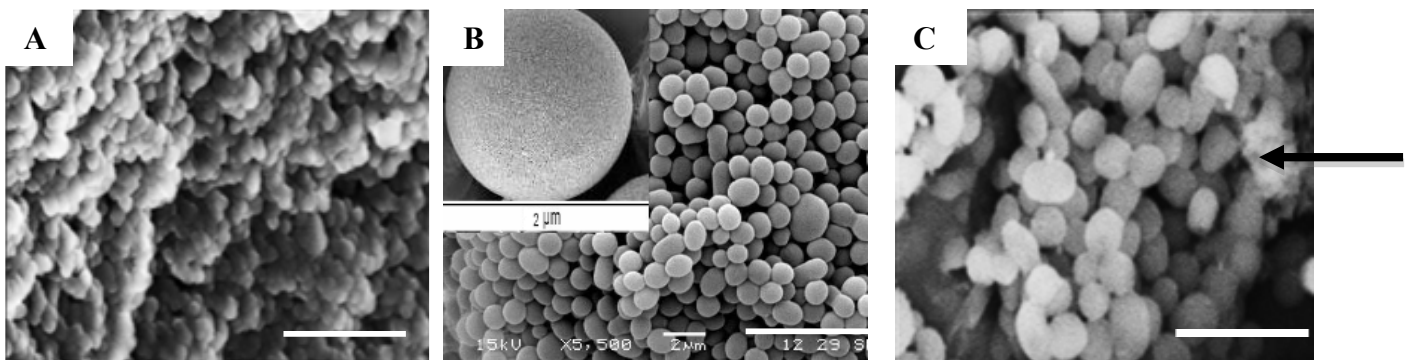


Figure 1. A) SEM image of n-BG particles. Scale bars = $100 \mu\text{m}$.
B) SEM image of P(3HB) microspheres. Scale bars = $2 \mu\text{m}$.
C) SEM image of P(3HB)/n-BG composite microspheres. Scale bars = $2 \mu\text{m}$.

For this study, n-BG particles which has surface area that is higher than that of microbio glass (m-BG) ($<1 \text{ m}^2\text{g}^{-1}$).³ These particles were also smooth, spherical in shape as compared to the irregularly shaped m-BG particles. The spherical morphology, with smooth regular shaped agglomerate sizes of bioactive glass particles have been found to influence the rates of HA deposition as well as to improve its haemostatic efficacy.⁹ The spherical morphology, large pore volume and a higher surface area are thought to facilitate the cation release required for both HA depositions as well as for contact activated coagulation.⁹ Ostomel⁹ have also

demonstrated the accelerated deposition rates of HA formation when mesoporous bioactive glass (MBGMs) particles with a high surface area were used. SEM images of P(3HB)/n-BG composite microspheres revealed the presence of n-BG particles attached on the surface of the microspheres. In a similar study, Qiu²⁵ also encapsulated modified bioactive glass (MBG) powders into polylactic acid (PLA) microspheres using a solid-oil-in water (s/o/w) technique. The surface morphology of the composite microspheres when analysed using SEM revealed the presence of MBG on the polymeric matrix.²⁵

Surface roughness (White light interferometry)

White light interferometry was performed on the samples to analyze the change in the surface roughness induced by the presence of n-BG particles when compared to the neat P(3HB) microsphere films as seen in Fig 2. This technique measures the surface roughness of a flat substrate; therefore, P(3HB) microsphere films and P(3HB)/n-BG composite microsphere films (diameter = 12.87 mm, thickness= 0.87 mm) were measured for changes in surface roughness. The rms roughness value of the composite microsphere films was measured to be 4.05 μm (Fig 2B) which was significantly ($n=3$, $**p<0.01$) higher than 3.79 μm (Fig 2A) measured for the neat P(3HB) microsphere films .

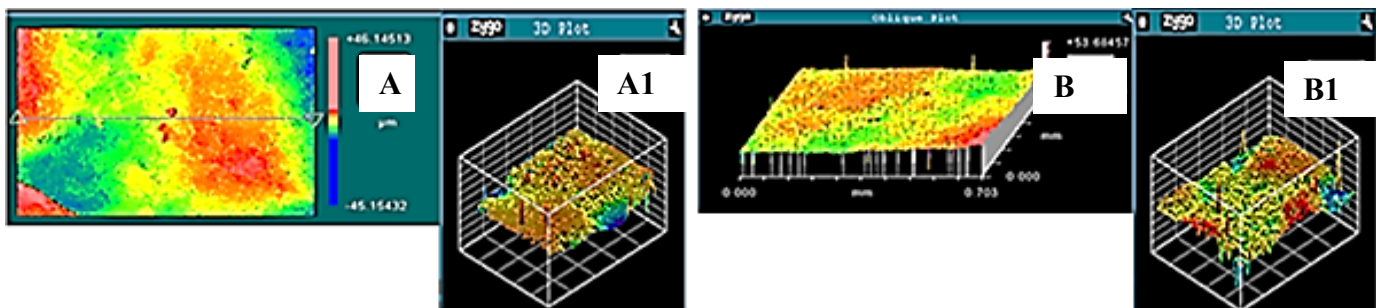


Figure 2. 2D and 3D plots of the P(3HB) microsphere film surfaces and P(3HB)/n-BG composite microsphere films as determined by white light interferometry. 2D plot (A) and 3D plot (A1) of the P(3HB) microsphere films. 2D plot (B) and 3D plot (B1) of the P(3HB)/n-BG composite microsphere films

White light interferometry was performed on the samples to analyze the change in the surface roughness induced by the presence of n-BG particles when compared to the P(3HB) microsphere films. A possible reason for the increase in the surface roughness of the P(3HB)/n-BG composite microsphere films could be the presence of n-BG agglomerations on the surface of the microspheres. After fabrication of the P(3HB)/n-BG composite microspheres, some

amount of n-BG particles that were not encapsulated within the microspheres could have possibly settled on the surface of the fabricated microspheres. These n-BG particles would have then bound to the surface of the composite microspheres due to physical interlocking. In a relevant study, Misra²⁰ examined the surface morphology of P(3HB)/n-BG composite solvent cast films using SEM, where they observed that the n-BG particles even after sonication agglomerated onto the surface of the films thereby inducing a rough topography to the films.²⁰ For wound healing applications the presence of the n-BG particles on the surface would be advantageous as both biomineralization and blood clotting are surface-mediated phenomena. Also, the presence of n-BG particles on the surface of the microspheres would induce nanoscale topography which can enhance attachment of cells required for wound healing.

Surface wettability

Static contact angle measurements of the P(3HB) microsphere films and P(3HB)/n-BG composite microsphere films were carried out to measure the surface wettability of the microsphere films, as shown in Fig 3. P(3HB) microsphere films had a contact angle of 60.9° and the composite P(3HB)/nBG microsphere films had a contact angle of 56.89° (n=3 *** $p < 0.001$).

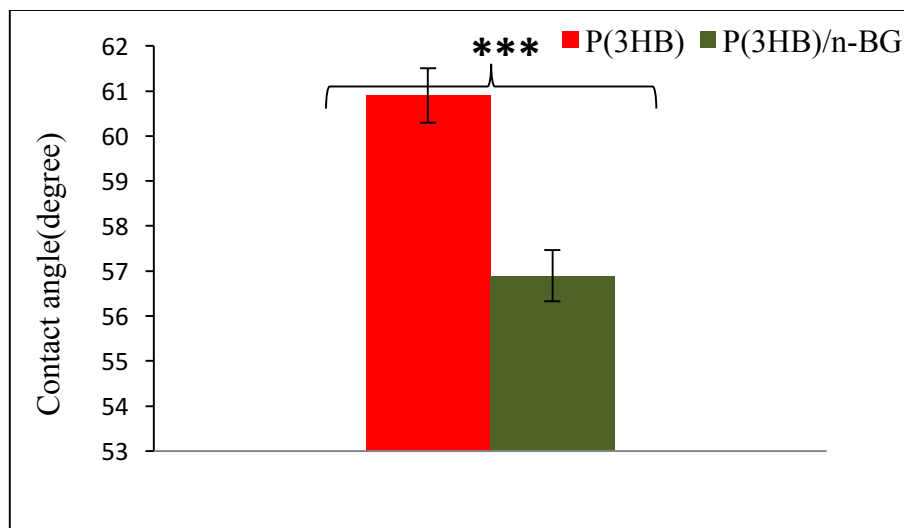


Figure 3. A comparison of the surface wettabilities of P(3HB) microsphere films and P(3HB)/n-BG composite films. The data (n=3; error bars= \pm s.d) were compared using t-test and the differences were considered significant when, * $p < 0.05$, ** $p < 0.01$ and * $p < 0.001$.**

Static contact angle measurements of P(3HB) microsphere films and P(3HB)/n-BG composite microsphere films were carried out to measure the surface wettability of the microsphere films. From the results, it is confirmed the surface wettability of the films had increased in the P(3HB)/n-BG composite microsphere films when compared to the P(3HB) microsphere films. The presence of the n-BG particles on the surface had increased the hydrophilicity of the P(3HB)/n-BG composite microsphere films due to which the water adsorption of the films had also increased.¹¹ In a similar observation made by Misra *et al.* 2008,¹¹ the presence of n-BG particles in the P(3HB)/n-BG composite microsphere films had improved the surface wettability of the films considerably. The water contact angle determined in this study for the P(3HB) films was lower than the value of $70 \pm 5^\circ$ measured by Wang *et al.*²⁹ Possibly, the presence of the hydrophilic PVA used to fabricate the microspheres influenced the surface wettability of the P(3HB) films thereby increasing the hydrophilicity.

Protein adsorption test

The protein adsorption study showed that the total amount of protein adsorbed on the surface of the P(3HB)/n-BG composite microsphere films before immersion in SBF was $323.5 \mu\text{g}$ which was higher than the value measured for the protein adsorbed on the P(3HB) microsphere films. Hence, the presence of the n-BG particles resulted in higher protein binding when compared to the P(3HB) microsphere films, as shown in Fig 4.

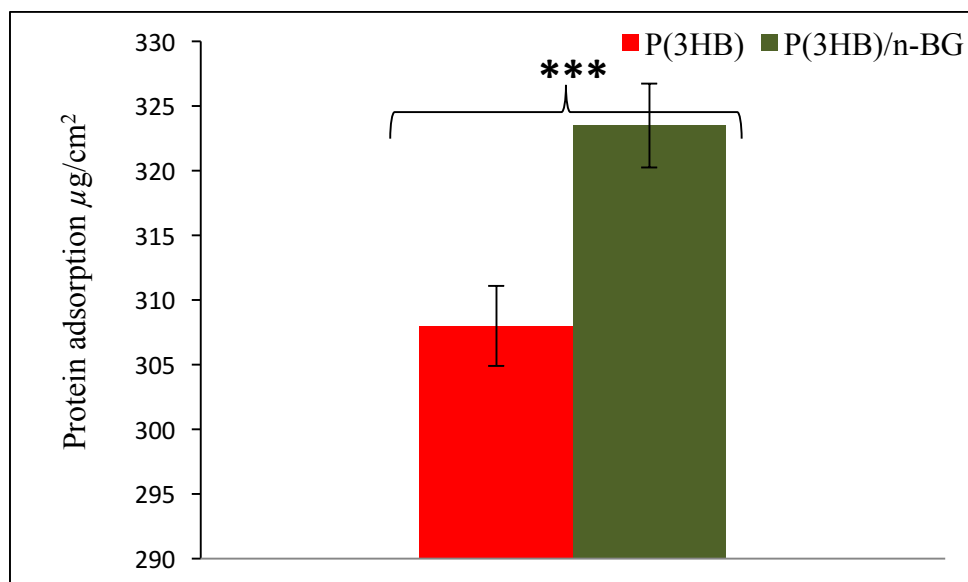


Figure 4. Total protein adsorption test carried out on the surface of P(3HB) microsphere films and P(3HB)/n-BG composites microsphere films. The data (n=3; data= \pm s.d) were

compared using t-test and the differences were considered significant when $*p<0.05$, $p<0.01$ and $***p<0.001$.**

This difference can be attributed to the effect of surface roughness on the P(3HB)/n-BG composite microsphere films caused by the presence of n-BG particles when compared to the neat P(3HB) microsphere films. This result is in agreement with the observation made by Misra¹¹ where the total protein adsorption was significantly higher (171 μ g) on P(3HB/n-BG) composite films when compared to the neat P(3HB) films. This difference in the protein adsorption was attributed to the marked differences in surface morphology, hydrophilicity and surface area available for protein adsorption.³ The presence of proteins on the surface of a biomaterial is known to promote the subsequent adhesion of cells on the biomaterial surface.

21

Cytocompatibility tests

Cell attachment tests performed using HaCaT cells, the keratinocyte cell line, on P(3HB) and P(3HB)/n-BG composite microsphere films, proved the cytocompatibility of the films. The results are shown in Fig 5.

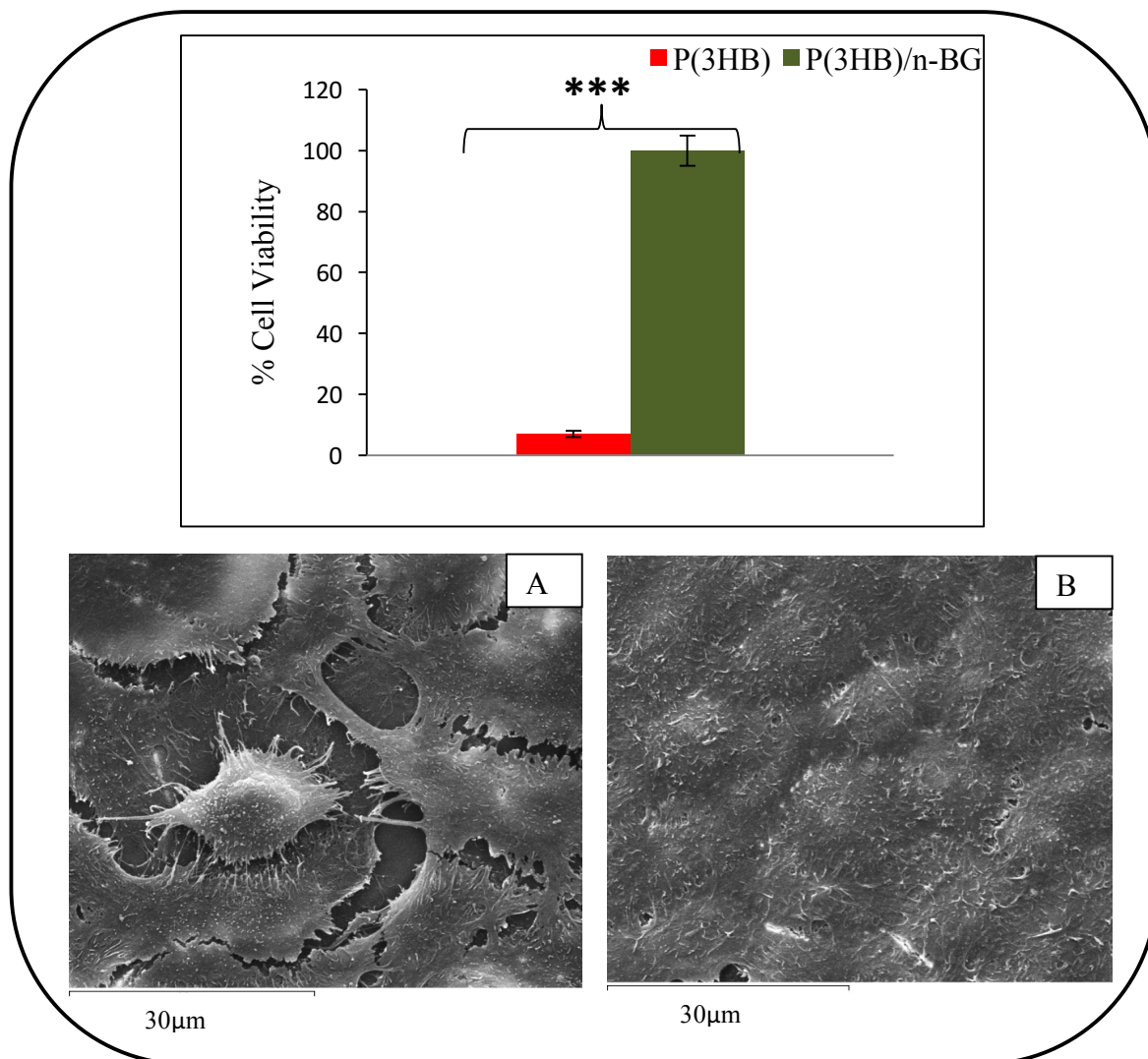


Figure 5. Cell viability studies performed on day 3, using Neutral Red assay, on P(3HB) microsphere films and P(3HB)/n-BG composite microsphere films. The data (n=3; data= \pm s.d) were compared using the t-test and the differences were considered significant when, $*p < 0.05$, $p < 0.01$ and $***p < 0.001$. SEM images of HaCaT cell attachment seen on day 3, on the surface of A) P(3HB) microsphere films and B) P(3HB)/n-BG composite microsphere films.**

The viability of the HaCaT cells on the P(3HB)/n-BG composite microsphere films was 100% which was a significant increase (n=3, $***p < 0.001$) when compared to the cell viability on

neat P(3HB) microsphere films which was only 7% (Fig 5). The % cell viability results in this study revealed a higher cell attachment on the P(3HB)/n-BG composite microsphere films when compared to the P(3HB) microsphere films. In this study, the nanotopography induced by the presence of n-BG particles as well as an increased protein adsorption contributed to the higher cell attachment on the P(3HB)/n-BG microsphere films as compared to the P(3HB) microsphere films. Misra¹¹ observed an increase of 65% in the proliferation rate of MG-63 osteoblast cell line when compared to the control (tissue culture plastic).³ The nano-protrusions formed on the P(3HB)/n-BG composite microsphere films in this study had also increased the surface area for cell-substratum contact and at this protrusion height (Fig 5B), the focal adhesion was not perturbed, as they were also able to trap the proteins that were necessary to increase cell adhesion. This behaviour also establishes the fact that the height of the nanotopographical feature is very critical; as this determines whether the adherent cells were exclusively located on the apex of the nanotopographical feature or if they were able to establish contact with the basal substrate and the other cells.¹⁵ The presence of n-BG thus notably improves the biocompatibility of P(3HB) microsphere films. The P(3HB) microsphere films on the other hand displayed a hydrophobic surface and lower cell adhesion ability (Fig 5A). Generally cells seeded on to a hydrophobic surface do not adhere onto the surface, thus resulting in a loose attachment.³¹

Haemostatic activity of n-BG

Nanoscale bioactive glass particles (n-BG) similar to those used here have been known to be haemostatically active, promoting the rapid formation of blood clots.⁹ Therefore, in this study, the *in vitro* haemostatic activity of varying amounts of n-BG particles (1mg, 2mg and 4mg) was evaluated using a TEG, is a clinical instrument used to monitor the change in the viscoelasticity of blood during clot formation (Fig 6).⁹ The initial detection of blood clot formation is referred to as R minutes. This is the time when the amplitude of bimodal symmetric viscoelasticity curve is 2mm. For example, when 1mg of n-BG particles were used, the R value was 7.7 min, for 2mg, the R value was 4.2 min and for 4mg, the R value was 3.8 min when compared to the control (in the absence of n-BG particles), which was 10.4 min.

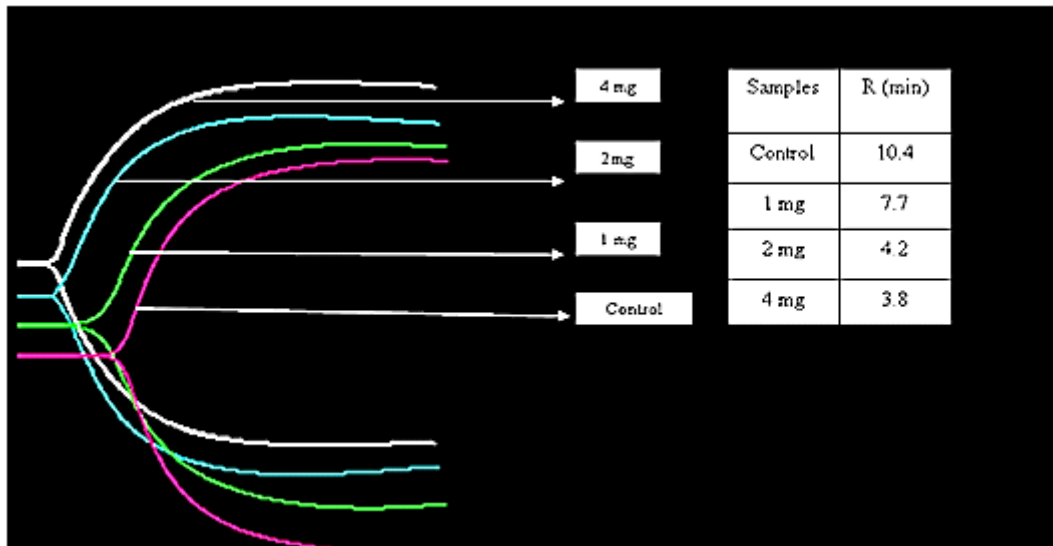


Figure 6. Thromboelastograph plot depicting the haemostatic activity of n-BG particles. The differences in the rate of coagulation in the presence of different amounts of n-BG particles were compared to the rate of coagulation in the control (absence of n-BG particles).

Nanoscale bioactive glass particles (n-BG) similar to those used here have been reported to be haemostatically active, promoting the rapid formation of blood clots.⁹ Ca^{2+} ions are responsible for a cascade of reactions that lead to fibrin polymerization and clot stabilization.¹⁰ Bioactive glasses are also known to be a rapid acting haemostatic agent as they release Ca^{2+} ions upon hydration.⁹ In the thromboelastograph tests it was observed that the time for clot detection had decreased linearly with the increase in the concentration of n-BG particles. These results were similar to the observation made by Ostomel⁹ where the clot detection time was seen to decrease linearly when the concentration of mesoporous bioactive glass (MBGM 80) was increased. In our study, the time for the clot formation, in the presence of n-BG particles, was much less when compared to those of the m-BG particles. The n-BG particles, as mentioned earlier, have a higher specific surface area of $79 \text{ m}^2\text{g}^{-1}$ when compared to m-BG ($<1 \text{ m}^2\text{g}^{-1}$). Hence, a reduced time for clot detection was observed in the presence of nBG.

P(3HB)/n-BG composite microsphere films immersed in SBF.

A composite film containing bioactive glass is considered to be bioactive largely due to its ability to nucleate new layers of HA at the implant-tissue interface when in contact with

physiological fluids.¹¹ The presence of an apatite layer on a biomaterial is also known to induce nanotopography. In addition, the surface chemistry of the apatite layer immersed for different time periods in SBF is known to vary. These variations in the biomaterial surface properties are known to have a significant effect on protein adsorption and the subsequent cellular interactions. Therefore, for this study, the P(3HB)/n-BG composite microsphere films were immersed in SBF, which is known to have an ionic composition similar to that of blood plasma for a period of 1, 3 and 7 days to induce the formation of an apatite layer. This bioactive layer was characterized using a range of techniques such as SEM/EDX and XRD analysis. Finally, the total protein adsorption on the surface of these composite films and the effect of this nanotopography on the keratinocyte attachment, morphology and proliferation was investigated.

Surface morphology

In order to further enhance the nanoscale topographical features such as surface roughness on the P(3HB)/n-BG composite microsphere films, they were immersed in SBF for a period of 1, 3 and 7 days to induce the formation of crystalline HA as seen in the SEM images (Fig 7). The surface of the P(3HB)/n-BG composite microsphere films on day 3 and day 7 (Fig 7c and d) revealed rough and uneven surfaces as compared to the films on day 1 which appeared fairly uniform and smooth (Fig 7b).

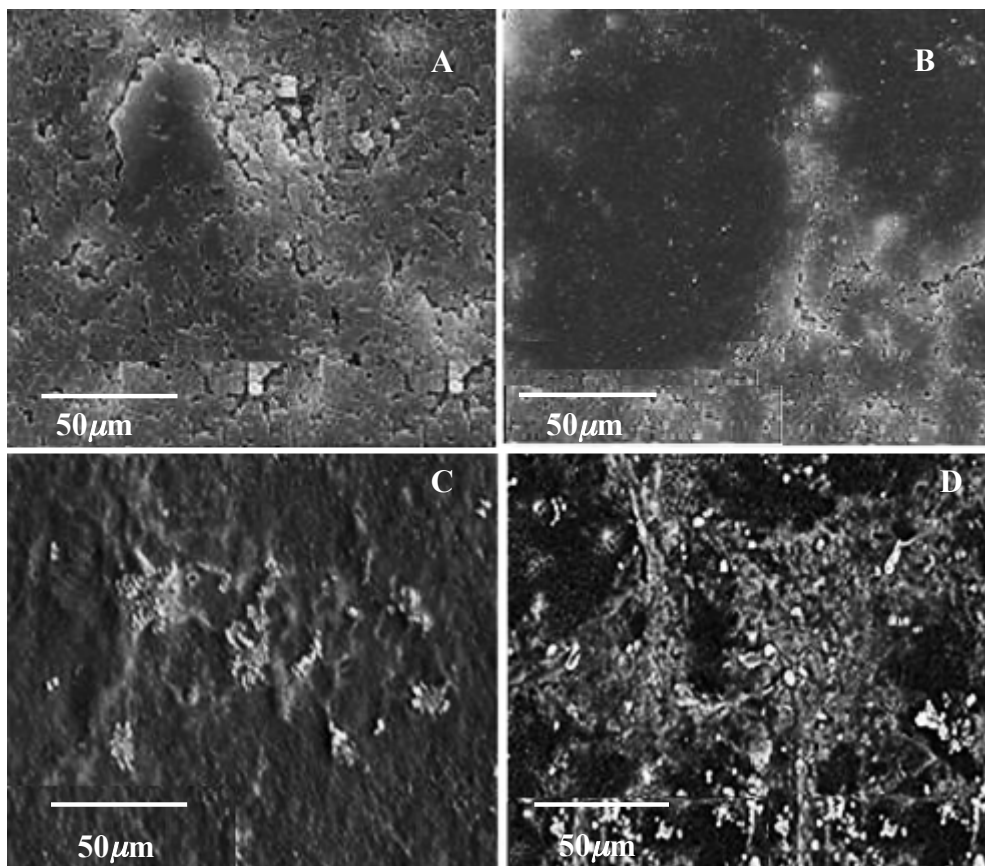


Figure 7. SEM images of the P(3HB)/n-BG composite microsphere films before immersion in SBF and after immersion in SBF. a) P(3HB)/n-BG composite microsphere film b) P(3HB)/n-BG composite microsphere film immersed in SBF for 1 day c) P(3HB)/n-BG composite microsphere films immersed in SBF for 3 days d) P(3HB)/n-BG composite microsphere films immersed in SBF for 7 days.

As seen from the SEM images, the surface morphology of P(3HB)/n-BG composite microsphere films before immersion in SBF was fairly uniform in appearance. The surface morphology of films immersed in SBF for 1 day was also comparable to films before immersion. However the nucleation of HA from the n-BG particles was evident from SEM micrographs of films immersed for 3 and 7 days. The presence of spherical nodules scattered over the surface was observed on the films immersed for 3 days. However, a more or less homogenous layer of HA crystals were observed on day 7 probably due to the presence of higher amount of n-BG particles on the surface.¹¹

Scanning Electron Micrographs/Energy Dispersive X-Ray (SEM/EDX) and X-Ray diffraction (XRD) analysis of P(3HB)/nBG composite microsphere films

The P(3HB)/nBG composite microsphere films when immersed in SBF for a period of 1, 3 and 7 days were analyzed using SEM/EDX analysis to highlight the transition of the nanoscaled bioactive glass particles to a calcium phosphate layer (Fig 8). From the EDX analysis of the composite microsphere films, the presence of Ca and P peaks was observed after immersion in SBF for a period of 1, 3 and 7 days, as seen in Fig 8 a, b, and c, although the Si peak was found on all the composite films, the intensity of the peak appeared to diminish after 3 days of immersion in SBF, as seen in Fig 8b.

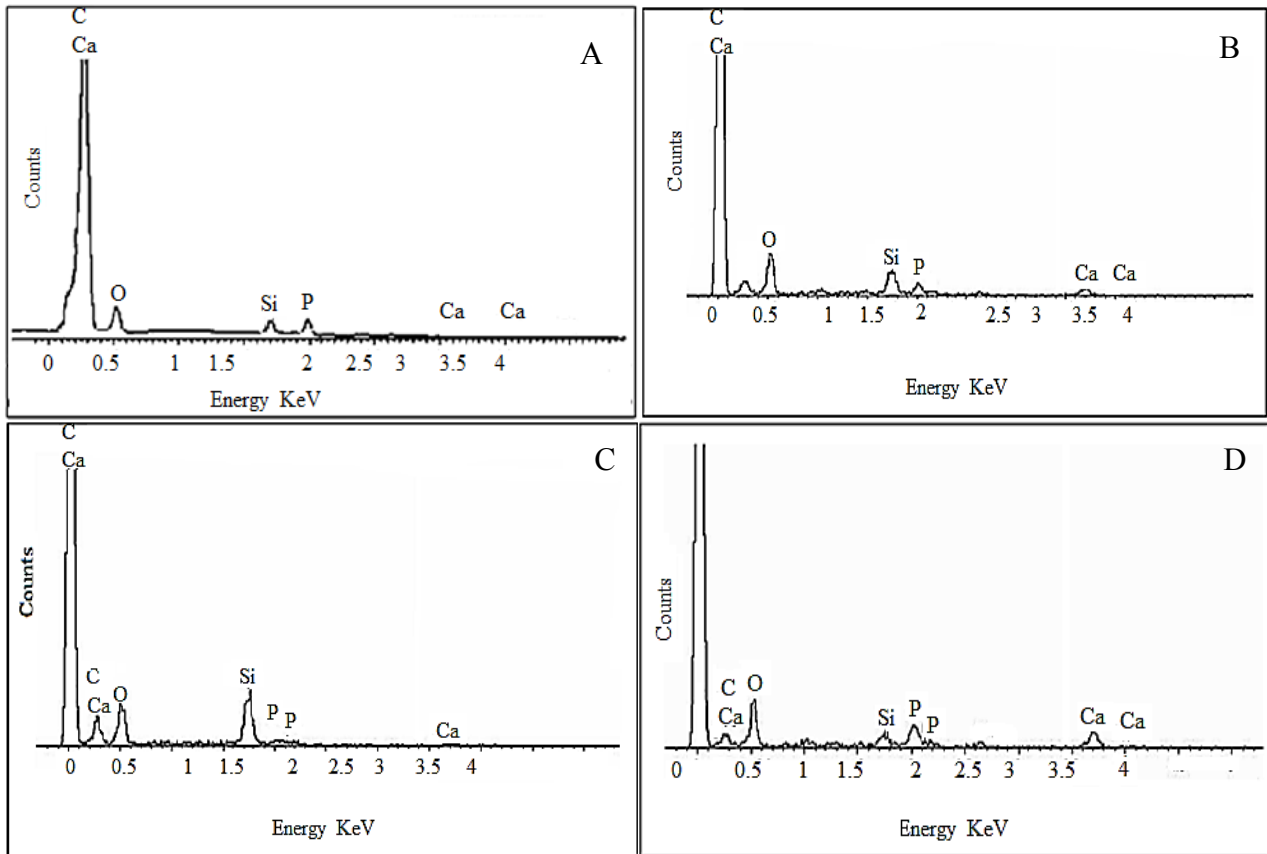


Figure 8. SEM/EDX results from P(3HB)/n-BG composite microsphere films after immersion in SBF for periods of 1, 3 and 7 days. a) The presence of Si, Ca and P peaks are observed. b) The relative intensity of the Si, Ca and P peaks appear increased on the surface of the P(3HB)/n-BG composite films after 3 days of immersion in SBF. c) On day 7, on the surface of P(3HB)/n-BG composite microsphere films. a decrease in the Si peak was observed, followed by an increase in the Ca and P peak.

The results of the EDX analysis of this study revealed the presence of Ca and P deposits on the films on day 1. These surface deposits contained high concentrations of Ca and Si initially but were low in P concentrations. All samples were initially high in Si concentrations but began to diminish after 3 days. Similarly, increases in the P concentrations were also observed with the increase in immersion time.

The X-ray diffraction peaks of the P(3HB)/n-BG composite microsphere films are shown in Fig 9. The growth of the characteristic crystalline HA peak between 2θ 31° and 33° was observed on P(3HB)/n-BG composite films when immersed in SBF for 1, 3 and 7 days, as seen in Fig 9. Thus the observations made from the SEM/EDX and XRD analysis are summarized as follows (i) characteristic crystalline HA peak between 2θ 31° and 33° was observed on the

P(3HB)/n-BG composite microsphere films after 1, 3 and 7 days of immersion in SBF (ii) the HA peak was shown to increase on prolonging the immersion time in SBF, indicating the transformation of amorphous (or weakly crystalline) HA to crystalline HA.

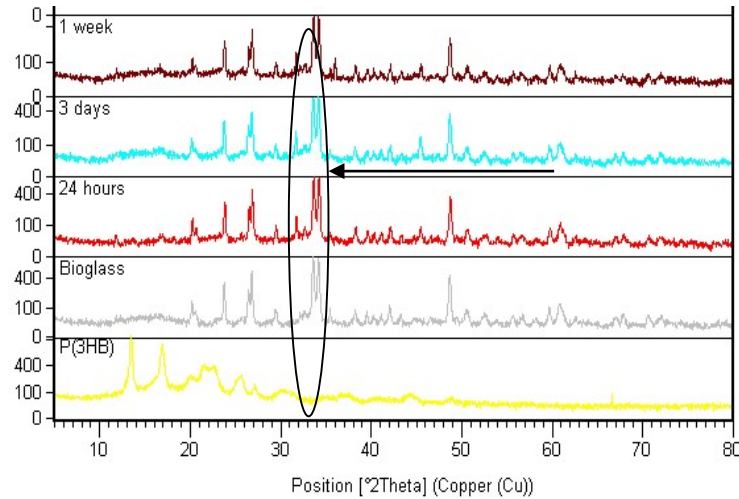


Figure 9. X-ray diffractograms of the P(3HB)/n-BG composite microsphere films after immersion in SBF. The arrow shows the characteristic crystalline HA peak between 20, 31° and 33°.

The early levels of bioactivity were confirmed using FTIR and SEM/EDX analysis, the X-ray diffraction studies were carried out to identify the presence of a prominent HA peak. The results of XRD studies, confirmed the presence of HA. The corresponding peaks at 2θ of 32° were found to increase with immersion in SBF. Misra¹¹ also observed a relative increase in the HA peaks at 2θ of 32° , of P(3HB)/n-BG, with an increased immersion time in SBF.¹¹ Thus from the results of the characterizations (FTIR, SEM/EDX and XRD) done in this study it can be concluded that the P(3HB)/n-BG composite microsphere films are bioactive in the presence of n-BG particles that significantly enhanced the surface reactivity of the P(3HB)/n-BG composites. The high level of exposure of n-BG particles on the film surfaces could have also contributed towards the enhanced bioactivity of the P(3HB)/n-BG composite microsphere films, thus transforming the inert polymeric surface into a highly bioactive surface.

Surface roughness (White light interferometry)

White light interferometry was performed to analyze the change in surface roughness of the P(3HB)/n-BG composite microsphere films induced by the presence of nanoscaled crystalline HA. The rms roughness value of P(3HB)/n-BG composite microsphere films on day 1 of

immersion in SBF was $4.3\mu\text{m}$, on day 3 was $5.99\mu\text{m}$ and on day 7 was $7.2\mu\text{m}$ ($n=3$ $***p<0.001$) (Fig 10) as compared to much lower rms values of $4.04\mu\text{m}$ of the P(3HB)/n-BG composite microsphere films before immersion in SBF.

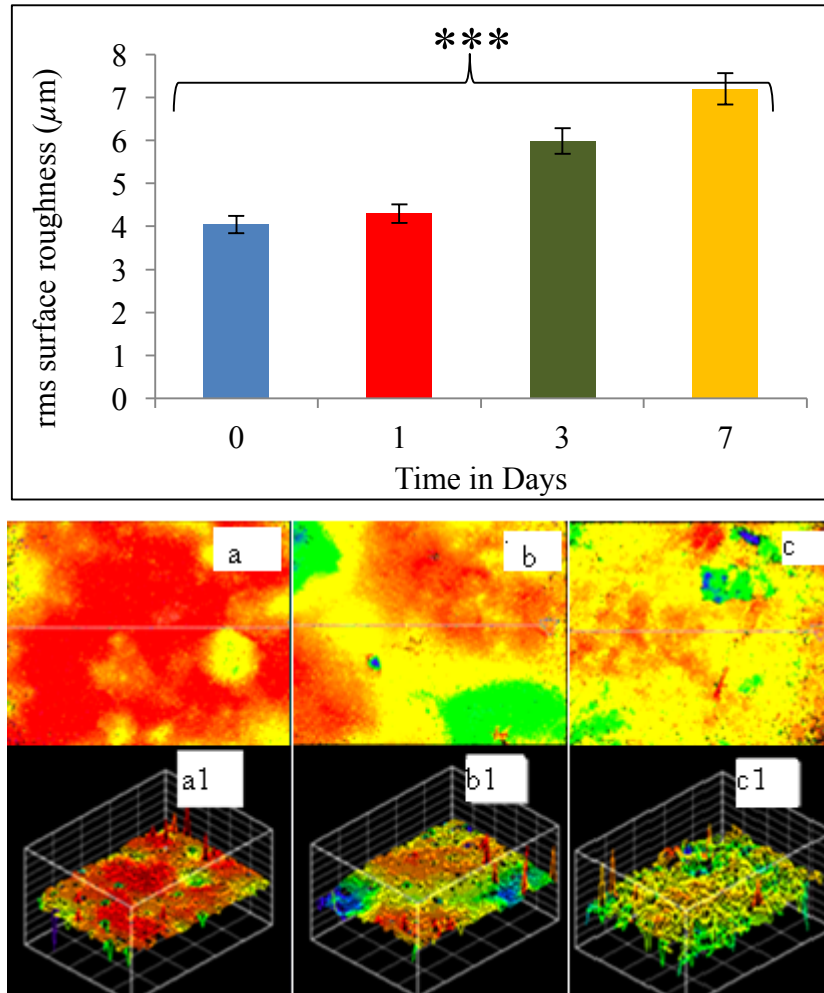


Figure 10. Quantification of the surface roughness of the P(3HB)/n-BG composite microsphere films after immersion in SBF for 1, 3 and 7 days measured using white light interferometry. 2D plot (a) and 3D plot (a1) of P(3HB)/n-BG composite microsphere films after immersion in SBF for 1 day, 2D plot (b) and 3D plot (b1) after immersion in SBF for 3 days, 2D plot (c) and 3D plot (c1) after immersion in SBF for 7 days. The data ($n=3$; $\text{data}=\pm\text{s.d}$) were compared using t-test and the differences were considered significant when $*p<0.05$, $p<0.01$ and $***p<0.001$.**

The surface roughness of the P(3HB)/n-BG composite microspheres immersed in SBF for 1, 3 and 7 days was analyzed using white light interferometry to study the changes induced in the

roughness due to the formation of crystalline HA. The surface roughness of the films on day 1 was comparable to the rms roughness values of films before immersion in SBF. SEM images confirmed this observation, where fairly uniform and smooth surfaces were observed. However, films immersed in SBF for 3 and 7 days, revealed an increasing surface roughness when compared to the films before immersion. As observed from the SEM images, the presence of spherical nodules on day 3 and a non-uniform layer of HA on day 7 had contributed to the changes in the surface roughness. The surface roughness maps along with the 2D plots of P(3HB)/n-BG composite films immersed in SBF for 3 days and 7 days did not reveal a homogenous roughness and there were some areas which exhibited higher relative roughness than the others. This non-homogenous surface roughness was again contributed by the lack of a uniform HA layer formed on day 3 and day 7. Similar results were observed in a study conducted previously, where the measured surface roughness values on day 7 for bioactive glass-ceramic pellets coated with microspheres after immersion in SBF was much higher as compared to the uncoated bioactive glass-ceramic pellets. The growth of HA crystals upon immersion in SBF was suggested to be responsible for inducing changes in the surface roughness of bioactive glass-ceramic pellets coated with P(3HB)microspheres.³²

3.3.5 Surface wettability

The static contact angle measurements on P(3HB)/n-BG composite microsphere films before and after immersion in SBF were compared to monitor the changes in surface wettability in the presence of the nanoscaled crystalline HA. The surface wettabilities of P(3HB)/n-BG composite microsphere films after immersion in SBF increased significantly ($n=3$ *** $p<0.001$) as compared to the composite microsphere films before immersion as seen in Fig 11. A decrease in the water contact angle of composite microspheres films observed on 1, 3 and 7 days was 12.60%, 19.29%, and 22.62%, respectively, when compared to the P(3HB)/n-BG composite microsphere films before immersion in SBF.

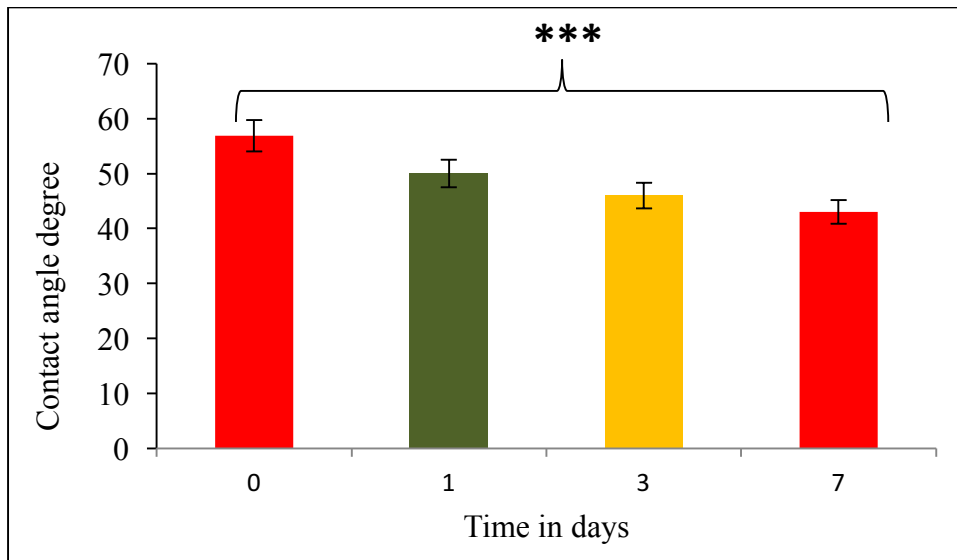


Figure 11. A comparison of the surface wettability of the P(3HB)/n-BG composite films before and after immersion in SBF on day 1, day 3 and day 7. The data (n=3; data= \pm s.d) were compared using t-test and the differences were considered significant when $*p < 0.05$, $p < 0.01$ and $***p < 0.001$.**

The presence of HA crystals on the surface of the P(3HB)/n-BG composite microsphere films led to a significant increase in the wettability of the composite films by lowering the water contact angle. The presence of the amorphous calcium phosphate deposition on day 1 and nanoscale sized HA crystals on day 3 and day 7 had thus improved the surface wettability of the films due to the increased hydrophilicity.

Protein adsorption test

In this study, the effect of the nanoscaled crystalline HA and its surface charge on protein adsorption was also investigated. The protein adsorption on the P(3HB)/n-BG composite microsphere films after immersion in SBF exhibited a lower amount of protein adsorption when compared to the composite microsphere films before immersion, as seen in Fig 12. For example, the composite microsphere films exhibited a 28% decrease in protein adsorption on day 1; a decrease of 90% on day 3 and 88% on day 7, as compared to the P(3HB)/n-BG composite microsphere films before immersion in SBF.

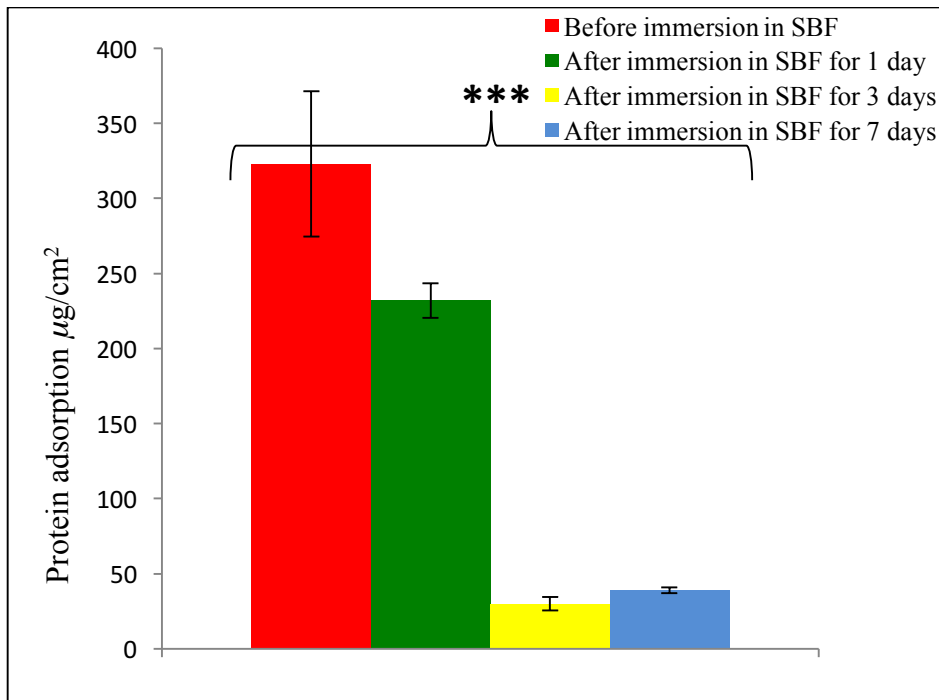


Figure 12. Total protein adsorption test carried out on the surface of P(3HB)/n-BG composites microsphere films (before and after immersion in SBF). The data (n=3; data= \pm s.d) were compared using t-test and the differences were considered significant when $*p<0.05$, $p<0.01$ and $***p<0.001$.**

Surface roughness is known to increase the potential surface area for cell attachment and biomaterial-cell interactions.³³ Thus the influence of HA formation on the total protein adsorption was investigated. P(3HB)/n-BG composite microsphere films before immersion in SBF were seen to exhibit the highest amount of protein adsorption as compared to the films after adsorption. The total protein adsorption on the P(3HB)/n-BG composite microsphere films after immersion was recorded the highest on day 1 and a small amount of protein adsorption was observed on day 7 and on day 3. This difference in protein adsorption on P(3HB)/n-BG composite microsphere films before and after immersion in SBF could be attributed to the surface charge, surface area, surface roughness and hydrophilicity variations induced by the formation of HA on the surface. Bioactive glass surface are known to carry an intrinsically negative surface charge (-14.72mV) analyzed using zeta-potential analysis³⁴ However, after immersion in SBF, the negative charge of the bioactive glass surface is neutralized by the adsorbed proteins.³⁴ On day 1 of immersion in SBF, the formation of an amorphous Ca-P layer is observed to induce a charge reversal from a negative to a positive

surface charge (7.47mV).³⁴ However, when an amorphous Ca-P layer is converted to a crystalline Ca-P layer with a prolonged immersion in SBF (3 days and 7 days), a second charge reversal from a positive (7.47 mV) to negative charge between -13 mV to -16.30 mV is observed to occur. This second sign reversal from a positive to negative charge occurs due to the precipitation of phosphate ions from the solution.³⁴ The nature of the zeta-potential charge of a material surface affects both the amount as well as the orientation of the proteins adsorbed.³⁴ Thus based on these observations, on day 1 of immersion in SBF the amorphous calcium phosphate layer carries a positive surface charge of 7.47 mV, therefore negatively charged protein molecules such as albumin, fibronectin and vitronectin present in Dulbecco's Modified Eagle medium (DMEM) bound to the surface, hence a higher amount of protein adsorption was observed when compared to the P(3HB)/n-BG composite films immersed in SBF for 3 and 7 days. On day 3 of immersion in SBF, the crystalline HA layer exhibited a surface charge of -13mV, which was higher than the negative charge of the P(3HB)/n-BG composite microsphere films before immersion, due to which less protein adsorption was observed. On day 7 of immersion in SBF, the films exhibited a higher negative surface charge of -16.30 mV when compared to the films on day 3 due to the precipitation of phosphate ions. Nevertheless a small amount of protein adsorption was also measured. Ghannam²¹ also observed a significant decrease from 1000 μ g to 800 μ g in serum protein adsorbed onto bioactive glass when the negativity of the material increased.²¹

Cell viability tests

Cell attachment tests performed using HaCaT cells, the keratinocyte cell line, on P(3HB)/n-BG composite microsphere films before and after immersion in SBF proved the biocompatibility of the films. A qualitative analysis of cell adhesion and distribution on P(3HB)/n-BG composite microsphere films was carried out using SEM. The results are presented in Fig 13.

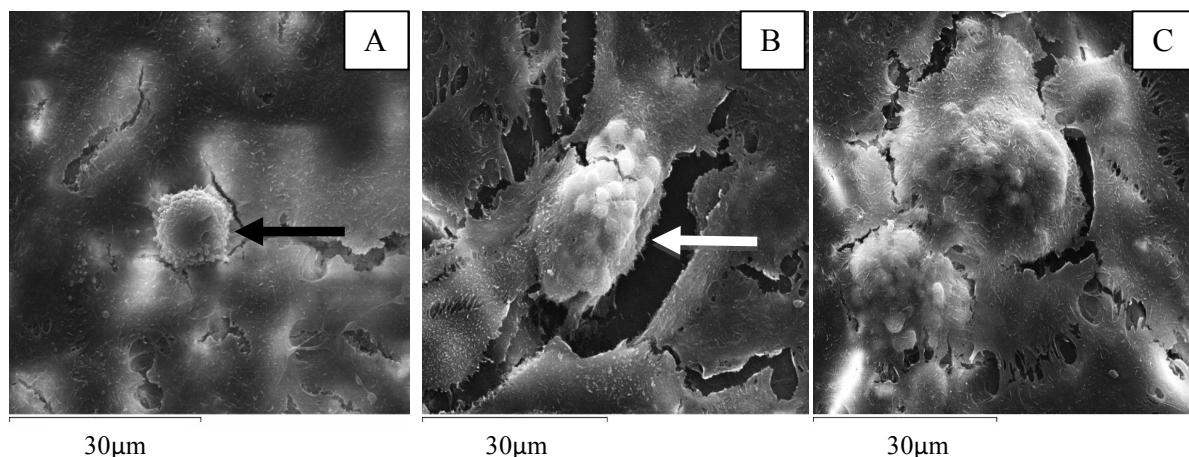
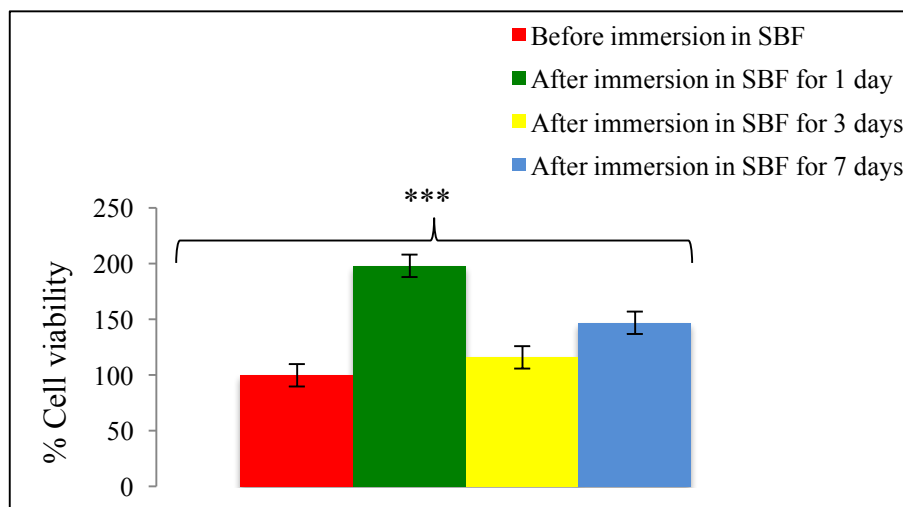


Figure 13. Cell viability studies performed on day 3, using Neutral Red assay, on P(3HB)/n-BG composite films. The test was carried out on films before and after immersion in SBF. The data ($n=3$; data= \pm s.d) were compared using t-test and the differences were considered significant when, $*p < 0.05$, $**p < 0.01$ and $***p < 0.001$. A) SEM images of HaCaT cell attachment seen on the surface of P(3HB)/n-BG composite microsphere films after immersion in SBF for 1 day. Similarly the HaCaT cell attachment is seen on P(3HB)/n-BG microsphere films immersed in SBF on days 3 and 7 are represented in Figs B and C.

The highest % cell viability was observed on the P(3HB)/n-BG composite microsphere films immersed in SBF for 1 day when compared to the % cell viability on the P(3HB)/n-BG composite microsphere films before immersion. The enhanced surface topography as well as an increased amount of protein adsorption might be one of the reasons why a significant increase in the % cell viability on the P(3HB)/n-BG composite microsphere films after immersion in SBF for 1 day was observed. These results were similar to the observations made by Ghannam²¹ where the highest adhesion of osteoblast (MC3T3-E1) cells was observed on the bioactive glass surface covered both by a layer of amorphous Ca/P and adsorbed serum protein when compared to other surfaces such as HA and bioactive glass (BG) with only protein and no amorphous Ca/P layer.²¹ In our study, the films immersed in SBF for 3 and 7 days also exhibited a significant increase in the % cell viability when compared to the % cell viability observed on films before immersion in SBF. Although a small-scale surface roughness between 10 nm to 10 μ m is suggested to influence biomaterial-cell interactions; an increase in surface roughness beyond an optimum point is also known to affect the cell interactions adversely.^{33,35} Thus the increased surface roughness of the films on day 3 and day 7 might had a negative effect on the % cell viability. The lesser amount of proteins adsorbed as well as the changes in the conformation of the adsorbed proteins on samples with higher surface roughness, after 3 and 7 days in SBF, may have contributed to the lower cell adhesion observed when compared to the cell adhesion on day 1.

SEM images of the HaCaT cells attached on day 1 on P(3HB)/n-BG composite microsphere films appeared to have a confluent layer of cell growth on the surface of the films comparable to the morphology of the cells attached on the P(3HB)/n-BG composite films before immersion in SBF (Fig 13A). Some cells were also seen growing on top of each other exhibiting limited space for them to spread. However, on day 3 and 7, the cells attached on the films appeared raised due to the formation of the scattered HA crystals on the surface of the composite films, as shown in Fig 13B and C. A significant increase in cell viability, expressed as a percentage of cell growth on tissue culture plastics, was observed on the P(3HB)/n-BG composite microsphere films after immersion in SBF when compared to the P(3HB)/n-BG composite microsphere films before immersion. The cell viability on films immersed in SBF for day 1 had increased to 198% followed by a decrease of 116% on films immersed for 3 days and of 147% on films immersed for 7 days. On day 1 a well-spread uniform surface morphology comparable to the cell attachment on the P(3HB)/n-BG microsphere films before immersion in SBF was revealed. The morphology of cells attached on the P(3HB)/n-BG composite

microsphere films that had been immersed for 3 days and 7 days in SBF appeared raised due to the presence of HA crystals beneath. The cells appeared to spread and form a non-uniform layer on the films. The surface irregularities of the films also seem to interfere with the cell attachment where a continuous uniform layer was not observed. Therefore, these results indicate that due to increase in surface roughness or nanotopography beyond an optimal value, cell attachment was affected due to which lower cell viability was recorded.³⁶ Although nanoscale protrusions act as mediators for cellular adhesions, protein adsorption and cellular differentiation, an increase in the nanoprotrusion height to 90 nm is known to cause a reduction in cellular adhesion for some cells such as human bone marrow stromal cells.³⁶ The cytoskeletal organization and the filipodia formation initially increase in the presence of an increased nanoscale protrusion when compared to the cells on a flat substrate. However, this attachment phase does not last for long and cells adhered on this protrusion undergo dedifferentiation or adhesion mediated apoptosis. Due to this, as a final result, a reduced cell adhesion or cell spreading is observed. Thus the results in this study were indicative of an increased nanoscaled protrusion (diameter and height) on the films immersed in SBF for 3 days and 7 days. Thus it can also be inferred that the nanoscaled features of the films immersed in SBF for 1 day were probably less than 60-70 nm in pillar height, which facilitated integrin clustering, and focal adhesion formation due to which a higher cell adhesion and enhanced cellular spreading occurred by providing tactile stimuli.³⁷ Thus from the results of the cell viability tests it was confirmed that P(3HB)/n-BG composite microsphere films immersed in SBF exhibited biocompatibility and lack of toxicity towards the HaCaT keratinocyte cell line. However, this study also revealed that there is an optimal point for increased surface roughness beyond which a negative effect on the cell-biomaterial interaction would be observed. The influence of varying surface properties such as surface chemistry and surface charge on the biocompatibility of the P(3HB)/n-BG composite microsphere films were also highlighted.

Conclusions

The effects of the presence of n-BG particles in P(3HB) microsphere films on the structural properties, thermal properties and biocompatibility of the films were studied. The nanoscaled bioactive glass with a high surface area was also assessed for its *in vitro* haemostatic efficacy and was able to successfully reduce the clot detection time. The surface roughness of the P(3HB)/n-BG composite microsphere films was increased by 5% when compared to the

P(3HB) microsphere films. Similarly an increase of 6.5% was observed in the surface wettability of the P(3HB)/n-BG composite microsphere films when compared to the P(3HB) microsphere films. The presence of the n-BG particles on the surface had increased the hydrophilicity of the P(3HB)/n-BG composite microsphere films due to which the water adsorption of the films had also increased. The total serum protein adsorbed and the cell proliferation rate on the composite microsphere films was significantly ($n=3$, $***p<0.001$) higher, when compared to the P(3HB) microsphere films before immersion in SBF. This difference was attributed to the effect of surface roughness.

It was also found that the nanotopography of the P(3HB)/n-BG composite microsphere films were further enhanced by the formation of HA on the surface of the composite microsphere films after immersion in SBF for periods of 1, 3 and 7 days. HA formation on the surface of the composite microsphere films was confirmed using FT-IR, SEM/EDX and XRD analysis. The results from these studies revealed a predominantly smooth amorphous calcium phosphate layer on the surface of the P(3HB)/n-BG composite microsphere films after 1 day of immersion in SBF when compared to the spherical nodules on the films immersed for 3 and 7 days which were analogous to that of apatite. This change in the nanotopography also had an influence on the surface roughness, surface wettability, protein adsorption and cell adhesion. The highest % cell viability (198%) was observed on films immersed in SBF for 1 day when compared to films immersed for 3 and 7 days which was 116% and 147%. An increased surface roughness of $5.99\mu\text{m}$ and $7.2\mu\text{m}$ of the films on day 3 and day 7 might have had a negative effect on the % cell viability. The composite microsphere films also exhibited a 28% decrease in protein adsorption on day 1; a decrease of 90% on day 3 and 88% on day 7, as compared to the P(3HB)/n-BG composite microsphere films before immersion in SBF. Thus the lesser amount of proteins adsorbed, as well higher surface roughness, after 3 and 7 days in SBF, may have contributed to the lower cell adhesion observed when compared to the cell adhesion on day 1. This study further indicated that there is an optimal surface roughness for increased cell adhesion beyond which it is deleterious for cell adhesion and differentiation.

Hence, in conclusion, this work has led to the development of novel P(3HB) composite microsphere films containing bioactive glass nanoparticles with great promise to be used for wound healing applications including protective, haemostatic and tissue regenerative properties, when engineered with optimal surface nanotopography.

Acknowledgements

We would like to thank the Scholarships Committee of the University of Westminster, London, UK for providing funding to support LF. We thank Prof. W. Stark and Dr D. Mohn, ETH Zurich for providing the nanoscale bioactive glass powder used in this investigation.

References:

1. Metcalfe AD, Ferguson MWJ, *J R Soc Interface* 4:413-437 (2007).
2. MacNeil S, *Nature* 445:874-880 (2007).
3. Seal BL, Otero TC, Panitch A, *Materials Science and Engineering* 34:147-230 (2001)
4. Greco KV, Francis L, Somasundaram M, Greco G, English NR, Roether JA, Boccaccini AR, Sibbons P, Ansari, T, *J Biomater Appl* 30(2):239-253 (2015)
5. Volova T, Shishatskaya E, Sevastianov V, Efremov S and Mogilnaya O, *Biochem Eng J* 16:125-133 (2003a).
6. Xiao X.Q, Zhao Y, Chen GQ, *Biomaterials* 28:3608-3616 (2007).
7. Valappil SP, Misra SK, Boccaccini AR, Keshvaraz T, Bucke C, Roy I, *J. Biotechnol.* 132:251-258 (2007).
8. Mourino V and Boccaccini AR, *J R Soc Interface* 7:209-227 (2009).
9. Ostomel TA, Shi Q, Tsung CK, Liang H, Stucky GD, *Small* 11:1261-1265 (2006).
10. Hoffman N and Rehm BHA, *FEMS Microbiol Lett* 237:1-7 (2004).
11. Misra SK, Mohn D, Brunner TJ, Stark WJ, Philip SE, Roy I, *Biomater* 12:1750-61 (2008).
12. Pramanik N, Bhargava P, Alam S, Pramanik P, *Polym Comp*, 27: 633-641(2006).
13. Teixeira AI, Nealey PF and Murphy CJ, *J Biomed Mat Res Part A* 71A (3): 369-376 (2004).
14. Norman J, *Biomed eng* 34:89-101 (2006).
15. Biggs MJP, Richards GR and Dalby MJ, *J Royal Soc Inter* 5:1231-1242 (2010).
16. Misra SK, Nazhat SN, Valappil SP, Moshrefi-Torbat M, Wood RJK, Roy I, Boccaccini AR, *Biomacro* 8:2112-2119 (2007).
17. Selhuber-Unkel M, Garcia L, Kessler H and Spatz JP, *Biophys J* 95:5424-5431 (2008).

18. Berry CC, Dalby MJ, Oreffo RO, McCloy D, Affrossman S, Curtis AS, *J Biomed Mater Res A* 79:431-439 (2006).
19. Webster TJ, Siegel RW and Bizios R, *Biomater* 20:221-227 (1999).
20. Misra SK, Philip SE, Chrzanowski NSN, Roy I, Knowles JC, Salih V, *J R Soc Inter*, 6:401-409 (2009).
21. El-Ghannam A, Ducheyne P and Shapiro M, *J Orthop Res* 17:340-345 (1999).
22. Prashar A, Locke IC and Evans CS, [Cell prolifer](#) 37: 221-229 (2002).
23. Shishatskaya El and Volova TG, *J Mat Sci:Mater Med* 15:915-923(2004).
24. Shih W-J, Chen Y-H, Shih C-J, Hon M-H, Wang M-C, *J Alloys and Comp* 434:826-829 (2007).
25. Qiu QQ, P. Ducheyne, P. Ayyaswamy, *J Biomed Mat Res* 52:66-76 (2000).
26. Valappil SP, Misra SK, Boccaccini AR, Keshavarz T, Bucke C, Roy I, *J Biotech* 132: 251-258 (2007).
27. Barba II, Salinas AJ, Vallet-Regí M, *J Biomed Mat Res* 47:243-250 (1999).
28. Wang C, Ye W, Zheng Y, Liu X, Tong Z, *Inter J of Pharma* 338:165-173 (2007).
29. Wang YW, Wu Q and Chen GQ, *Biomater* 24:4621-4629 (2003).
30. Misra SK, Ansari TI, Valappil SP, Mohn D, Philip SE, Stark WJ, Knowles JC, Salih V, Boccaccini AR, *Biomater* 31:2806. (2010).
31. Peschel G, Dahse H-M., Konrad A, Weiland GD, Mueller PJ, Martin DP, Roth M, *J Biomed Mater Res* 85 A:1072-1081 (2007).
32. Francis L, Meng D, Knowles JC, Roy I, Boccaccini AR, *Acta biomater* [6:2773-2786 \(2010\)](#).
33. Itälä A, Ylänen HO, Yrjans J, Heino T, Hentunen T, Hupa M. Aro HT, *J Biomed Mat Res* 62:404-411(2002).
34. Lu H, Solomon R, Pollack PD, *J Biomed Mater Res* 54:454-461 (2001).
35. Dowling PD, Miller IS, Ardhaoui M, Gallagher WM, *J Biomater Appl* 1:1-22 (2010).
36. Lee JH, Khang G, Lee JW and Lee HB, *J. Colloid Interface Sci* 205:323-330(1998).
37. Den BET, Ruijter JE De, Smits HT, Ginsel LA, Von Recum AF and Jansen JA, *Biomater*, 17:1093-1099 (1996).